Novel High Speed 3 DOF Linear Direct Drive Operating With Submicron Precision

Bernhard Sprenger [a], Roland Siegwart [b]

[a] Swiss Federal Institute of Technology Zurich (ETHZ) • Institute of Robotics
8092 Zurich, Switzerland • Email: sprenger@ifr.mavt.ethz.ch

[b] Swiss Federal Institute of Technology Lausanne (EPFL) • Institute of Microengineering
1015 Lausanne, Switzerland • Email: roland.siegwart@epfl.ch

Abstract

Developments in microelectronics, micromechanics and microelectromechanical systems (e.g. micromotors, microsensors) require significant improvements in manufacturing tools for mass productions. Especially the assembling tools have to become faster and more precise.
Many assembly devices use *XY* stages driven by DC servomotors with ball screws or parallel structures; others use linear drives with traditional ball bearings. Only a few devices use linear drives together with air bearings, but always together with an angular guide for *X* and *Y* direction.
The novel approach presented in this paper is based on linear drives together with a planar air bearing. In contrast to other stages, it doesn't need any angular guide. This reduces the moved mass and leads to higher accelerations. It consists of an arrangement of four identical moving-coils attached to a slide, which is suspended by a planar air bearing. This new configuration allows a workspace of 60 x 60 mm^2 and an acceleration exceeding 10 g[1] with a resolution better than 100 nm.
This paper gives an overview of the system, describes the design of the moving-coils and shows first experimental results of the controller.

Keywords: linear drive, actuator, 3 degree of freedom, air bearing

1. Introduction

The need for high speed and high precision positioning systems is increasing in many fields of technology, such as microelectronics [1], micromechanics and microelectromechanical systems. For mass production, the assembling/mounting tools have to achieve high precision and have to work with high speed or/and highly parallel.

There are many concepts to build high speed or high precision manipulators, but only a few of them can serve to obtain high speed together with high precision:

- Ball screw drives obtain high precision, but high speed can not be reached because of its large inertia and high friction.
- Impact drives [2] and inchworms achieve high resolution over a large working area, but only with low speed. Their main fields of application are the manipulation of small objects underneath microscopes (e.g. the manipulation of cells in science of medicine or biology) and near field microscopy.
- Fast parallel drives, similar to the Delta-Robot [3], have the advantage, that their motors are fixed and don't have to be moved. This reduces the moved mass and allows to achieve high acceleration. They use ball bearings for the joints, which have radial run-out of several µm. The inaccuracy is growing with each joint of the robot. Other problems are the low stiffness of these structures, the friction in the joints and the difficult kinematics and dynamics. All these effects make it difficult to achieve high precision together with large acceleration.
- Steel cables or steel belts as transmission elements allow the construction of high performance manipulators [4]. Their main advantage is, that their motors are fixed and don't have to be moved, which leads to minimal inertia of all moving

1. $1g = 9.81ms^{-2}$

parts. The attainable resolution is limited due to their vibrational properties, their complex deflection of cables/belts and their friction.

- Linear drives achieve high performance and good resolution, but their combination for multiple dof[1] is difficult to realize. They are often arranged to parallel structures by the use of angular guides [5]. The friction can be eliminated by air bearings, leading to an enhanced resolution [6]. The disadvantages of these solutions are their complex designs (e.g. 3 air bearings) and the large moved mass resulting from the angular guides.

A novel type of a 3 dof linear drive is presented in this paper. This approach consists of four identical moving coils attached to a slide. This slide glides on a granite plate and is suspended by one planar air-bearing. In contrast to other stages, it doesn't need any angular guide. The lack of angular guides reduces the moved mass, leading to higher acceleration. It also simplifies the mechanical construction. This design allows a workspace of 60 x 60 mm^2 and an acceleration exceeding 10 g with a resolution better than 100 nm.

This paper gives an overview of the system, describes the moving coil actuators and shows first experimental results. Mechanical and electromagnetic FEM simulations are used to layout the moving coils and to calculate the relation between current and force. To obtain an assessment about the dynamics, the electrical transfer function is measured and the eddy currents are estimated [7]. This assessment is needed to design the power amplifiers and, together with the characterization of the sensor system, to layout the control system. First experimental results are obtained by the use of a not optimized PD-controller, showing the possibility to control the system with respect to the constraints given by the sensor systems.

2. System Overview

Basic elements of the 3 dof linear-drive are its actuators (fig. 1), based on moving coils. Each of them consists of a merged arrangement of two traditional voice coils [8][9][10]. In the field of fast and precise positioning the main advantage of moving coils is that only the light coil moves whereas the heavy stator/core is fixed. In addition, the use of air bearings results in a frictionless design. This frictionless actuation and the linear current-force relation ease the controller design and increase the attainable precision.

The arrangement of bearings is done by one planar air bearing, which permits free movement in the *XY*-plain, whereas movements in *Z*-direction and rotations around *X*-/*Y*-axis are prevented. Therefore a minimum of three actuators are necessary to control these 3 dof. The advantage of uncoupled *XY*-measurement systems leads towards a rectangular configuration with three actuators. In order to avoid high torsion stress in the system and to increase its controllability and performance, a 4th actuator has been added, resulting in a more symmetrical, but redundant actuated system. The redundancy in actuation can easily be treated by the controller.

This desired mechanical setup is shown in fig. 2, its cross section in fig. 3. It consists of four identical moving coils attached to the slide, which glides on a granite plate suspended by the planar air-bearing. This bearing consists of pressure and vacuum zones, delivering high stiffness. Due to increase the accesibility to the sensor system for calibrating purpose, the system used for the first measurements and movements is equipped with only three actuators instead of four (fig. 4).

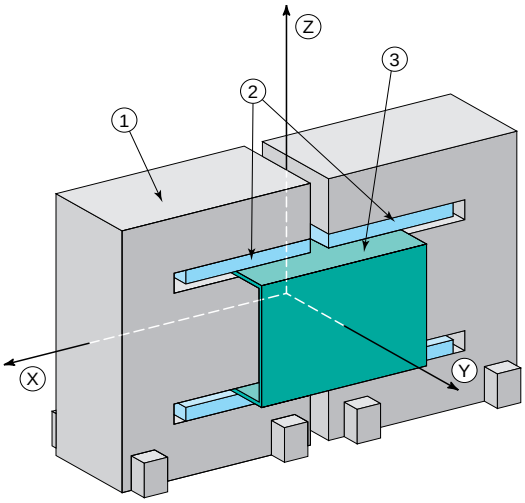

Fig. 1: Voice-Coil Type Actuator (1-Core/Stator, 2-Magnet, 3-Moving Coil)

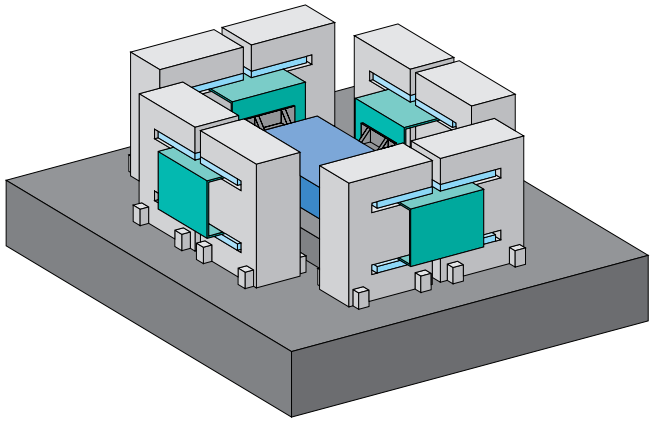

Fig. 2: 4 Actuator System Configuration

1. dof = degrees of freedom

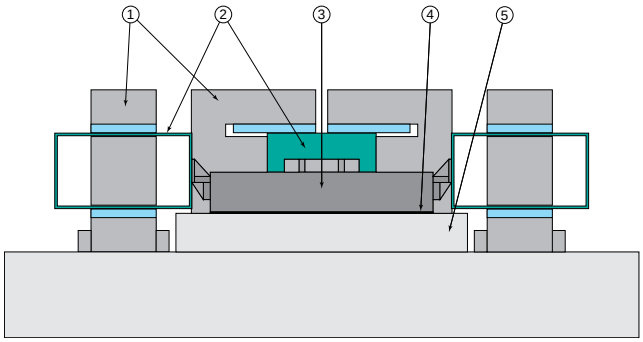

Fig. 3: Cross Section
(1-Core/Stator, 2-Moving Coil, 3-Slide,
4-Air Bearing, 5-Granite Plate

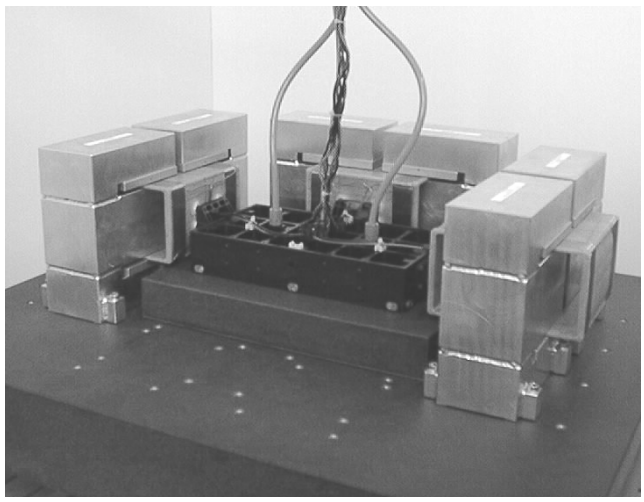

Fig. 4: 3 Actuator Experimental Setup

3. Design of the Actuators

The size and mass of the slide is conditioned by the used sensor system from *Heidenhain* and the required stiffness of the air bearing. Together with the coils and the tool, a mass of about 5 kg has to be accelerated. The proposed acceleration of 10 g demands that each actuator has to deliver a force of 250 N at a coil current of 8 A.

The design of the actuators consists of a merged arrangement of two commercial stators/cores from *ETEL* and a newly developed coil. The air gap (in which the coil moves) of these stators/cores limits the thickness and the allowable deformation of the coil. The coil has to adhere to this limit even at maximum force.

The coils are optimized by FEM simulations to fulfill these conditions (force, thickness and displacement) with minimal weight, maximal stiffness and large electromagnetic dynamics. The stiffness and the displacement are obtained from mechanical simulations, whereas the current-force relation is gained from electromagnetic simulations. The electrical transfer function is measured and the eddy currents are estimated to obtain an assessment about the dynamics of the electromagnetic system, which is essential to design the controller and power amplifier.

3.1. Electromagnetic FEM Simulation

Because 3D FEM simulations require huge computer resources, a reduced 2 dimensional model is used for the electromagnetic simulations. The expected errors resulting from this reduction are smaller than the spread of the magnets (± 5%). The model of the actuator (fig. 5) consists of a merged arrangement of two voice coils, allowing to produce high force with small leakage of flux and little mass to be moved.

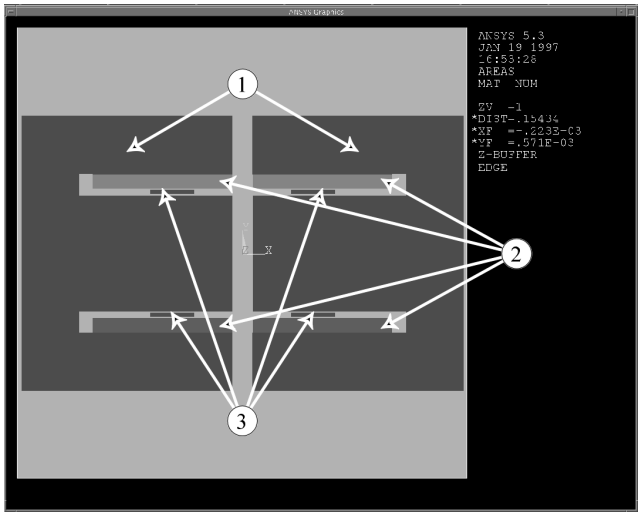

Fig. 5: Electromagnetic Simulation Model
(1-Core/Stator, 2-Magnet, 3-Moving Coil)

Each of these coils consists of 120 windings arranged in 3 layers. Applying a coil current of 8 A results in a force of 254 N. The resulting magnetic flux density is shown in fig. 6 and the magnetic field lines are shown in fig. 7.

These figures show a small field displacement into the left core of the actuator, leading to a field weakening through the coils. This effect ensues from the small air gap between the two cores. The smaller this air gap gets the bigger the field displacement and the field weakening through the coils becomes. Because the resulting force is a function of the magnetic flux through the coils, it is reduced by this displacement too. An enlargement of the air gap between the two cores reduces this effect but it also leads towards a bigger coil with more mass to move. As a consequence, the optimal distance between the two cores is found to be about twice the gap (including the height of the magnets) in which the coil moves. The resulting force of 254 N is about 5% underneath its theoretical maximum, which would be reached with an infinite gap between the cores.

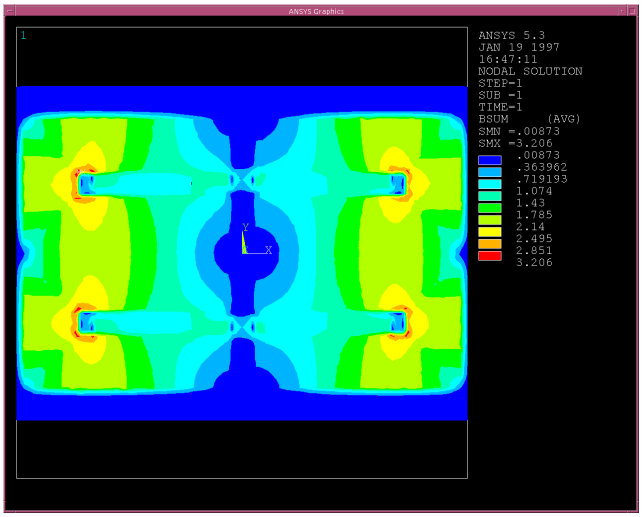

Fig. 6: Magnetic Flux Density

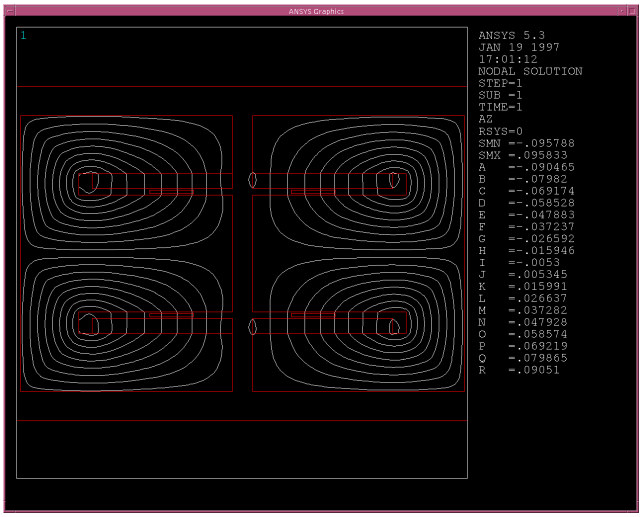

Fig. 7: Magnetic Field Lines

The current-force relation is obtained by FEM-simulations and verified by measurements. This relation is linear as expected and is shown in fig. 8.

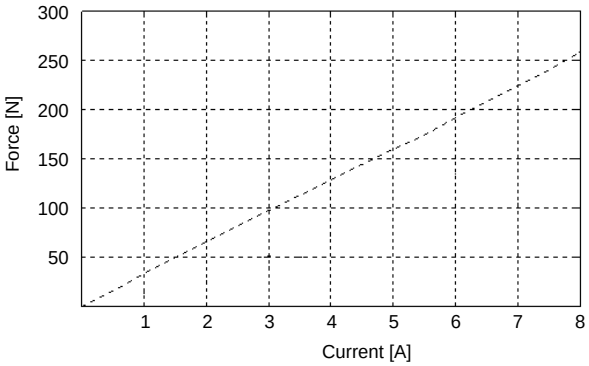

Fig. 8: Measured Current-Force Relation

3.2. Mechanical FEM Simulation

One important condition for the mechanical design is the height of the air gap, in which the coil moves. This limits the allowable deformation of the coil. Another important condition is that the stress in the fiber glass doesn't exceed the material limits. To fulfill these conditions the design of the coils has been optimized by mechanical FEM simulations, leading to a solution with enhanced thickness of the lamination at the side walls, which are not in the air gap.

The employed 3 dimensional model for these mechanical FEM simulations is shown in fig. 9. Applying the maximum load of 254 N results in the displacement shown in fig. 10. The maximum values of the displacement in *X*-, *Y*- and *Z*-direction are listed in tab. 1. This elasticity has to be treated by an intelligent controller design.

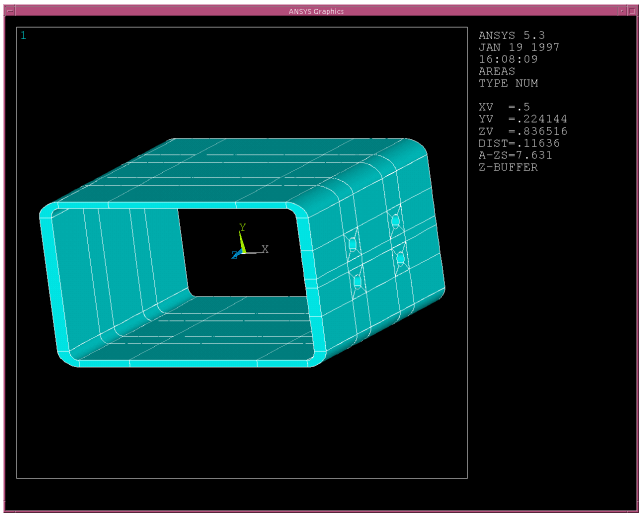

Fig. 9: Mechanical Simulation Model

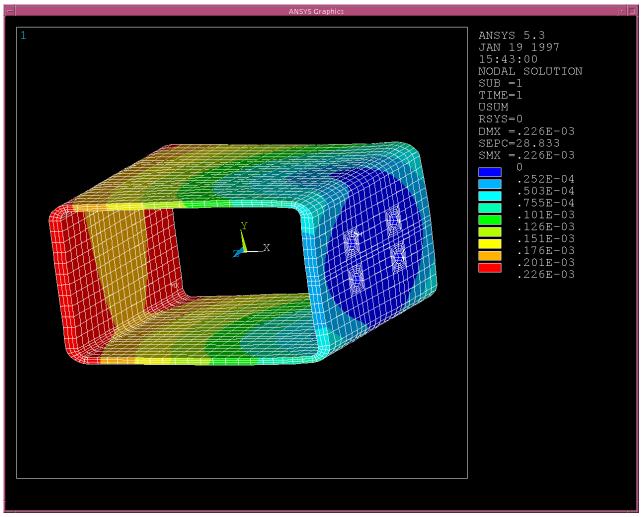

Fig. 10: Displacement

Direction	Displacement (mm)
X	< 0.153
Y	< 0.056
Z	< 0.226

Tab. 1: Maximal Displacements

3.3. Electrical Model and Eddy Currents

For the design of the controller and power amplifier it is essential to know the electromagnetic dynamics of the actuator. First of all the electrical transfer function is measured, the electric conduction ($P_n = Real\left[\frac{1}{z}\right]$) calculated and an estimation about the eddy currents is made [7].

The electrical transfer function of the moving coil actuator is measured with the coil fixed to its core/stator and is shown in fig. 11. Due to a mechanical mode of the coil structure, the electrical transfer function shows a small resonance at ~ 105 Hz, that can be neglected for the following considerations.

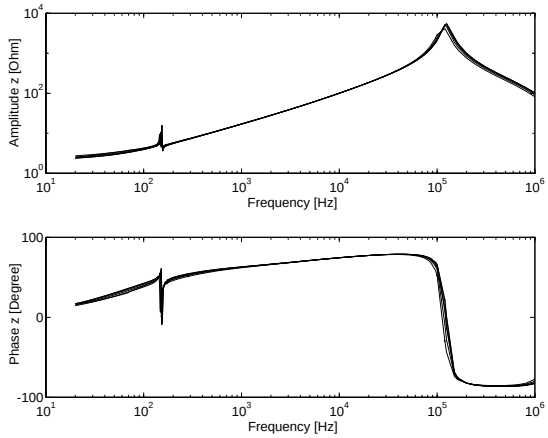

Fig. 11: Electrical Transfer Function

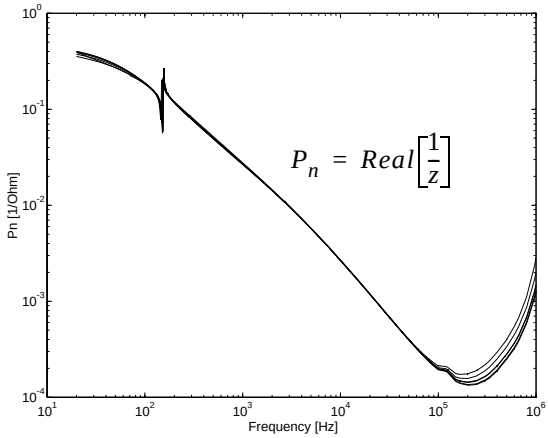

Fig. 12: Electric Conductance Function

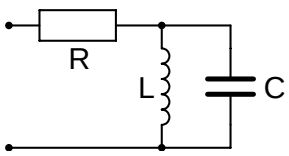

$$z = R + \frac{j\omega L}{1 - \omega^2 LC}$$

Fig. 13: Equivalent Circuit

The complex impedance of the actuator shows an ohmic behaviour (phase ~ 0) for low frequencies due to the resistance of the wires, an inductive behaviour (phase ~ $\pi/2$) for frequencies up 100 kHz due to the coil inductance, a resonance at 100 kHz and a capacitive behaviour (phase ~ $-\pi/2$) for frequencies over 100 kHz due to the capacity between the windings. This leads towards the equivalent electrical circuit for the coil shown in fig. 13, which consists of a resistor, an inductance and a capacity.

Eddy currents are one of the main effects, that limit the dynamics of electromagnetic actuators. For high frequencies they lead to huge losses in the core and even inside the wires. Dominating eddy currents are characterized by an electrical transfer functions with a phase near to $\pi/4$. Analyzing the transfer function (fig. 11) leads to the assessment, that they can be neglected in the shown frequency range and that the electromagnetic dynamics of the actuators exceed 200 kHz. The use of an high speed controller together with a ultra fast switching amplifier is reasonable.

Similar considerations about the eddy current can be done using the electric conductance function shown in fig. 12. The loss of the actuator is evaluated by the conductance and the applied alternating voltage:

$$P_l = P_n \cdot U^2$$

Accordingly the electric conductance function can be interpreted as the normalized loss function. The conductance function shows a decreasing behaviour up to 200 kHz, which is identical with decreasing losses. The increasing conductance for frequencies over 200 kHz results from the capacity between the windings, which acts like a short circuit for high frequencies. Dominating eddy currents would be represented by exploding losses (conductance) for high frequencies. Therefore the eddy currents can be neglected at least up to 200 kHz and the electromagnetic dynamics certainly exceed 200 kHz.

4. Control System

One main requirement upon the control performance ensues from the used commercial sensor system. This sensor system allows only tiny rotations of less than ±1.5 mrad. The sensor system and its characterization is discussed in chap. 4.1. The controllability of the linear drive together with the limitations of the sensor system is proofed by the implementation of a simple preliminary PD-controller on the real system. The structure and step function of this preliminary controller are presented in chap. 4.2.

4.1. Sensor System

Due to the lack of a sensor system delivering both the *XY*-position as well as the rotational angle with the demanded accuracy, a combination of 2 commercial available two-coordinate sensor systems is used instead. These sensor systems are incremental two-coordinate grid plate encoders from *Heidenhain*, each delivering an accurate *XY*-position with a resolution better than 100 nm. The rotational angle around the *Z*-axis is obtained from these two positions together with the distance between the two sensor systems, resulting in a rotational resolution better than 10 µrad.

Due to their physical principle, these sensors allow only a tiny rotational displacement (around the Z-axis) between the sensor head and the grid plate. This dependency between the amplitude of the delivered encoder signals (sinusoidal form) and the rotational displacement around the *Z*-axis is shown by fig. 14.

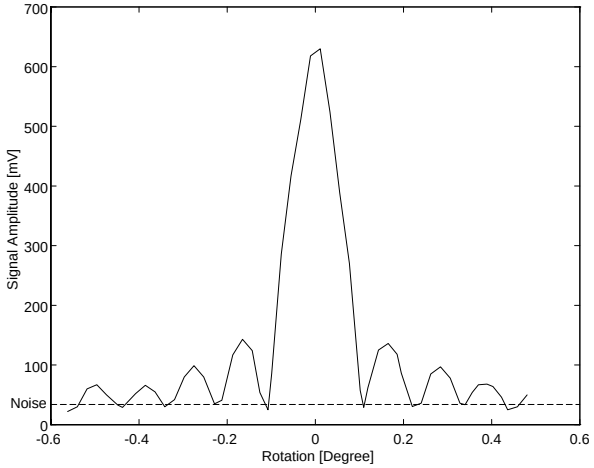

Fig. 14: Ampitude-Rotation Sensitivity

This amplitude-rotation relation is quite similar to a sinc^2-function. Its generation can be explained by the moire effect between the grid plate and the reference grid due to rotational displacement. Because of the zeros in this function, the usability of these sensor systems is limited to rotational displacements of less than ±1.5 mrad (±0.1 °). The amplitude information is eas-

ily extracted out of the 90° phase shift encoder signals ($\cos^2+\sin^2=1$) and therefore it will also be used by the controller to toggle the emergency stop, when the slide leaves the allowed rotational range.

4.2. Control Structure

To proof the possibility to control a system with these restrictions, a simple preliminary PD-controller is realized, leading to first results. Due to increase the accesibility to the sensor system for calibrating purpose, the system used for the first measurements and movements is equipped with only three actuators instead of four. This more unsymmetrical structure leads to smaller control accuracy, but it also requires a more robust controller and can be used as a harder proof for controllability.

The implemented control structure is shown in fig. 15. The plant is modeled as a rigid and not as a flexible structure; its mass and inertia are roughly estimated. Due to this inexact modelation and due to a not optimized PD-controller design, the reachable control performance is strongly limited. The corresponding step response of this preliminary controller is shown in fig. 16 and fig. 17.

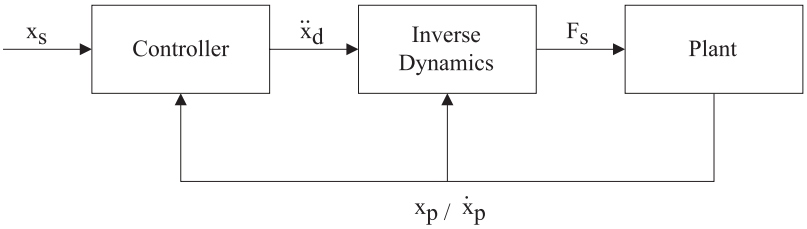

Fig. 15: Control Structure

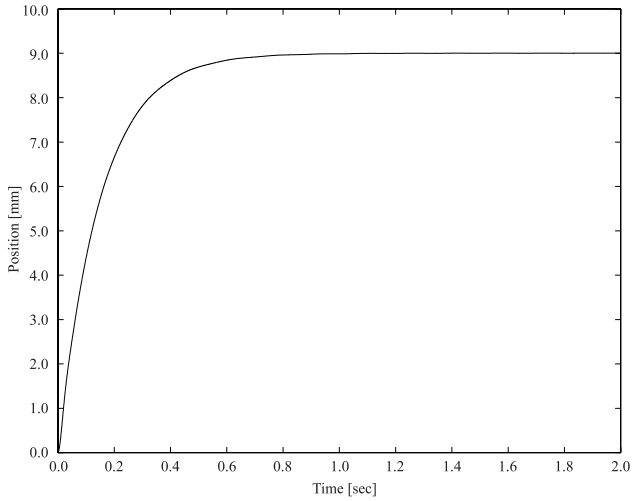

Fig. 16: Transitional Step Response

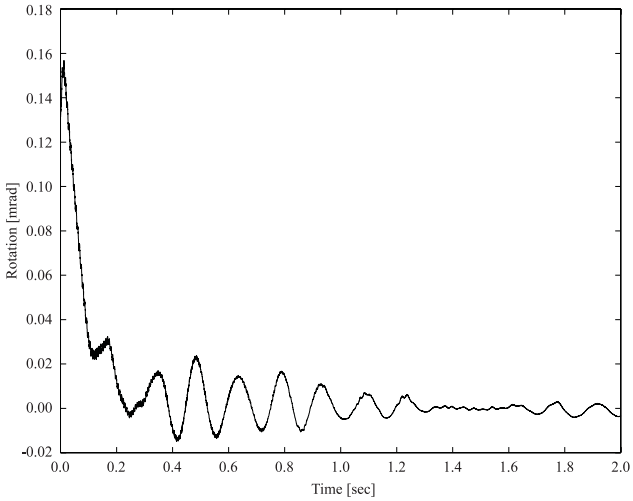

Fig. 17: Rotational Step Response

The step responses show, the feasibility to control the system even with this simple not optimized PD-controller. The controller will be improved by the invocation of a precise model, a model predictive design and with the introduction of acceleration sensors.

5. Conclusions

A new design of a linear drive is introduced in this paper, which is based on traditional voice coils. It allows a work space of 60 x 60 mm^2 with a sensor resolution better than 100 nm. This drive is a wear-resistant, maintenance-free and frictionless design because of its air bearing. Its electromagnetic dynamics exceeds 200 kHz, allowing the use of an high speed controller together with a ultra fast switching amplifier. The possibility to control such a system with the restriction given from the used sensor system is shown by the implementation of a simple PD-controller. The project goals of an acceleration exceeding 10 g with a repeatable precision of 100 nm require an improved controller design, which has to be developed by future work.

6. References

[1] W. Beckenbaugh, “Manufacturing Implications of Ultra High Speed Packaging and Interconnect Design”, *Fourth IEEE/CHMT European International Electronic Manufacturing Technology Symposium Proceedings*, pp. 108-111, 1988.

[2] W. Zesch, R. Büchi, A. Codourey and R. Siegwart, “Inertial Drives for Micro- and Nanorobots: Two Novel Mechanisms”, *SPIE Microrobotics and Micromechanical Systems*, Philadelphia, USA, pp. 80-88, October 1995.

[3] R. Clavel, “DELTA, a Fast Robot with Parallel Geometry”, *Int. Symp. on Industrial Robots (ISIR)*, pp. 91-100, 1988.

[4] H. Fässler, H. A. Beyer and J. Wen, “Robot Ping Pong Player. Optimized Mechanics, High Performance 3D Vision, and Intelligent Sensor Control”, *Robotersysteme*, Vol. 6, No. 3, pp. 161-170, 1990.

[5] O. Masamitsu, H. Toyomi and W. Mitsuhito, “High Speed and High Accuracy XY-Stage for Electronic Assembly”, *Fourth IEEE/CHMT European International Electronic Manufacturing Technology Symposium, Proceedings*, pp. 104-107, 1988.

[6] C. Meisser, H. Eggenschwiler and W. Nehls, “Einrichtung zur Durchführung der Zustellbewegung eines Arbeitsorgans zu einer Arbeitsstation”, *European Patent Application No. 0317787B1*, ESEC SA, 1988.

[7] L. Kucera and M. Ahrens, “A Model for Axial Magnetic Bearings including Eddy Currents”, *Third International Symposium on Magnetic Suspension Technology*, Tallahassee, USA, pp. 421-436, 1995.

[8] G.W. McLean, “Review of Recent Progress in Linear Motors”, *IEE Proceedings Part B v 135*, pp. 380-416, 1988.

[9] J. Stupak and G. Gogue, “Voice-Coil Actuators: Insight into the Design”, *Intelligent Motion*, pp. 241-253, October 1989.

[10] B. Black, M. Lopez and A. Morcos, “Basics of Voice Coil Actuators”, *PCIM*, pp. 44-46, July 1993.